Geochemistry Geophysics Geosystems G3
AN ELECTRONIC JOURNAL OF THE EARTH SCIENCES
Published by AGU and the Geochemical Society

Article
Volume 3, Number 8
6 August 2002
10.1029/2002GC000300
ISSN: 1525-2027

Power spectrum of sea level change over fifteen decades of frequency

C. G. A. Harrison

Rosenstiel School of Marine and Atmospheric Science, University of Miami, 4600 Rickenbacker Causeway, Miami, Florida 33149, USA (charrison@rsmas.miami.edu; 305-361-4610)

[1] The power spectrum of relative sea level change has been estimated over more than 15 orders of magnitude in frequency, from a frequency of 1/(591 Ma) to a frequency of 1/(5 s). Although there are still regions of the spectrum where data sampling and duration do not allow the power to be calculated, most notably between periods of 100–1000 years, the general shape of the spectrum is that in which the power depends on the square of the reciprocal frequency, apart from periods between 1 and 100 years where the power spectrum falls off less steeply with increasing frequency. A spectrum in which power depends on reciprocal frequency squared is the same spectrum as that calculated from a random walk signal of finite length. There are some causes that have defined frequencies, such as those associated with tides and the Milankovitch cycles of the ice ages, but there is also a continuum of relative sea level change that requires other causes. The implications of this are discussed in the light of global change and heating of the lithosphere from the bottom.

Components: 8430 words, 10 figures, 3 tables.

Keywords: Sea level; spectra; random walk; ocean tide; epeirogeny.

Index Terms: 1206 Geodesy and Gravity: Crustal movements—interplate (8155); 1249 Geodesy and Gravity: Tides—Earth; 1699 Global Change: General or miscellaneous; 4556 Oceanography: Physical: Sea level variations.

Received 4 January 2002; **Revised** 22 April 2002; **Accepted** 23 April 2002; **Published** 6 August 2002.

Harrison, C. G. A., Power spectrum of sea level change over fifteen decades of frequency, *Geochem. Geophys. Geosyst.*, *3*(8), 10.1029/2002GC000300, 2002.

1. Introduction

[2] Sea level change is important in many fields. Over geological time, it can affect continental erosion and sediment deposition on the continental shelf. It can also control how much sediment is lost over the shelf break to the surrounding ocean basins. From a geological perspective the important timescale of sea level change is thousands of years and longer. Sea level variation on a shorter timescale is important from a human perspective as a possible factor in anthropogenic global change. It is well known that relative sea level is rising today and many people assume that this is due to anthropogenically produced global warming [*Baltuck et al.*, 1996]. However, it is possible that the changes seen over the recent past in tide gauge records are part of the natural signal. It is therefore important to understand as much as possible about the natural variations in sea level so that informed decisions may be made about the possibility of future human induced changes.

[3] *Agnew* [1992] has discussed the power spectra of several different types of signal. In particular, he has calculated the spectrum of sea level change for

Table 1. Sea Level Power Spectrum Estimates

Data Source[a]	Period range, a	Frequency Range, c/a	Frequency Band Width, c/a	Total Power, m^2	Power per Unit Band Width, $m^2/(c/a)$
1	$(4 \text{ to } 20) \times 10^7$	$(0.5 \text{ to } 2.5) \times 10^{-8}$	200×10^{-10}	4194	2.10×10^{11}
2	$(1 \text{ to } 50) \times 10^6$	$(0.02 \text{ to } 1) \times 10^{-6}$	98×10^{-8}	5000	5.10×10^9
3	$(0.2 \text{ to } 1) \times 10^6$	$(1 \text{ to } 5) \times 10^{-6}$	40×10^{-7}	757	1.89×10^8
4	$(1 \text{ to } 8) \times 10^3$	$(1.25 \text{ to } 10) \times 10^{-4}$	875×10^{-6}	8.41	9.61×10^3
5	10^2 to 10^4	$(1 \text{ to } 100) \times 10^{-4}$	99×10^{-4}	2	2.02×10^2

[a]1, Continental flooding; 2, oscillations of the western interior seaway; 3, Florida raised beaches; 4, Pacific sea level; 5, postglacial SL variations.

Honolulu over more than eight decades of frequency, from 10^{-9} Hz to 2×10^{-1} Hz. This is equivalent to periods between 5 s and 32 years. Over much of this range of periods or frequencies the power is related to the frequency with a spectral index of -2 ($\beta = 2$ [$-$spectral index] according to *Turcotte* [1997]). In other words, if the log of power is plotted against the log of frequency, the slope is -2. Peaks appear on this continuum spectrum at tidal periods (semidiurnal, diurnal, etc.) and also at monthly and semimonthly periods (also representing tides). At the high frequency end of the spectrum, there is a strong and broad peak centered on a period of 10 s, which represents wave action. There is also some enhanced power at periods of about an hour. At the long period end of the signal the spectrum flattens out (between periods of 32 years and ~6 years. Agnew's Figure 4 shows the spectrum as $10 \times \log_{10} P$ (where P is the power in m^2/Hz) plotted against the logarithm of frequency in Hz.

[4] In another paper I discussed the power spectrum over longer periods [*Harrison*, 1988]. The power was expressed as $\log_{10} P$ where P is power in m^2/cpmy (cycles per million years) plotted against $\log_{10}$(frequency in cpmy). The shortest period for which I presented data was 10 years or a frequency of 3.17×10^{-9} Hz. The longest period for which there were data was 200 my. Thus if this spectrum is combined with that of *Agnew* [1992] the frequency range spans close to 15 orders of magnitude. The spectrum by *Harrison* [1988] also had a spectral index of -2. The top left-hand corner of *Agnew*'s [1992] plot has coordinates of $10^6 m^2$/Hz and 10^{-9} Hz. These translate into $3.17 \times 10^{-8} m^2$/cpmy and 31,558 cpmy, allowing the two power spectra to be joined.

[5] Factors controlling changes of sea level change seen today are discussed at some length in *Church et al.* [2001]. The factors causing the largest changes are thermal expansion of ocean water, changes in volume of glaciers and ice caps including Greenland and Antarctica, and terrestrial storage. Some of these causes, and all other possible causes, have errors that are larger than the possible effect.

2. Data for the Sea Level Spectrum

[6] In this section, the two spectra will be joined together, and additional data will be added in the middle of the frequency range so as to fill in some of the gaps that were present in *Harrison*'s [1988] generalized spectrum. At the high frequency end of the spectrum the data came from bottom pressure gauges and tide gauges. At the low frequency end of the spectrum, the data came from geological information of various types. There was a significant range of periods where no data were available. Beginning with the smallest frequencies the individual spectral estimates will be discussed in more detail.

[7] The record for the longest periods (first entry in Table 1) is from a study of the amount of continental area flooded by marine waters as a function of time. The area so flooded records the relative variation in continental elevation with respect to the ocean surface. The area flooded is transformed into a relative sea level change by use of the hypsographic curve. This relative sea level fluctuates with time because of epeirogenic movements, ocean volume variations, and other effects [*Bond*, 1979; *Harrison et al.*, 1981; *Harrison*, 1988]. Ocean volume variations are eustatic and affect

all continents equally. Epeirogenic movements, however, affect individual continents or portions of continents. What these data represent is a combination of both. The data points are spaced every 20 Ma, and the length of each record is 200 Ma, giving the period and frequency bands shown in Table 1. Since the areas of flooding are measured on a continental scale, it can be assumed that higher frequency fluctuations, which will cover smaller areas, will be largely averaged out in these records of flooding area. This preliminary result has been expanded by doing power spectra for each continent and averaging the power from all continents at each frequency, giving the cluster of five square points shown in the top left hand corner of Figure 1. This average spectrum has a slope of −2.0 but with a large error because of scatter, the small number of points in the spectrum (5) giving a limited frequency range of a factor of 5.

[8] The data point for the next longest period in Table 1 is obtained from oscillations of sea water seen in the Western Interior Seaway [*Kauffman*, 1969], for which the data length is 50 Ma and each data point is spaced every 500 ka. This is a shallow water seaway covering parts of western North America that waxed and waned during the Jurassic and Cretaceous [*Barron et al.*, 1981]. Sea level fluctuations in the Western Interior Seaway are almost certainly not eustatic but epeirogenic [*Harrison*, 1985]. The third longest periodicity is obtained from a study of raised beaches in Florida, which record the uplift of the peninsula over the past 1 Ma, allowing the high stands of sea level of the interglacial periods to be recorded at different levels as time passes by. Data points occur every 100 ka. This signal is almost certainly an epeirogenic signal, relevant only to the Florida peninsula. Further details about these three data points are given by *Harrison* [1988].

[9] *Grossman and Fletcher* [1998] have produced a sea level curve for Oahu for the past 8000 years, showing a high stand of sea level 3 ka ago of almost 2 m. Analysis of this curve, assuming that the minimum frequency was 0.125 ka and the maximum frequency was 1 ka produced a total power of 8.41 m^2. This is entry 4 in Table 1 and has been added to Figure 1 but is almost entirely obscured by the high frequency portion of the SPECMAP spectrum. H. R. Wanless (personal communication, 2000) has suggested that over the past 10,000 years, the record of sea level as seen in sedimentary material available by coring on the continental shelves is equivalent to a sea level variation with an amplitude of about 2 m. The total power in this frequency range is then 2 m^2. This data point has been put into Table 1 (entry 5) and onto Figure 1.

[10] Part of the gap in the results presented by *Harrison* [1988] has been filled in by a sea level spectrum calculated from sedimentary sequences recorded in seismic profiles measured over the continental margin off the Spanish coast by *Hernandez-Molina et al.* [1994]. This record is 24,000 years long and extends to periods of less than 500 years, governed by the spacing of the data points in the record that was subjected to Fourier analysis. The power spectrum from this sequence stratigraphic record is shown in Figure 1. The spectral index of the record is about −1, but the record is relatively short so that the error in this slope estimate is quite large. The best fitting straight line through the spectrum is shown in Figure 1. The datum for the longest period was not available, so that the longest period plotted is 12,000 years. The data were read from a plot of linear power plotted against linear frequency. Power at very high frequency plotted close to the abscissa, rendering it difficult to read numbers close to, but not, zero, probably resulting in artificially high values of power for the high frequency end of this spectrum, and an unrealistically small value of β.

[11] A much longer record of sea level change covering a different part of the frequency spectrum but also derived from sedimentary sequences on continental margins is the Exxon/Haq sea level curve extending back 591 Ma [*Haq et al.*, 1987]. This sea level curve is illustrated in Figure 2 and consists of data points spaced every 0.1 Ma. The spectrum from this sea level record is shown in Figure 3, and it can be seen that the low frequency part of the spectrum has a slope of about −1.7, represented by the thick red line, whereas the higher frequency end of the spectrum as a slope of −2.3, shown by the thick blue line, the separation being

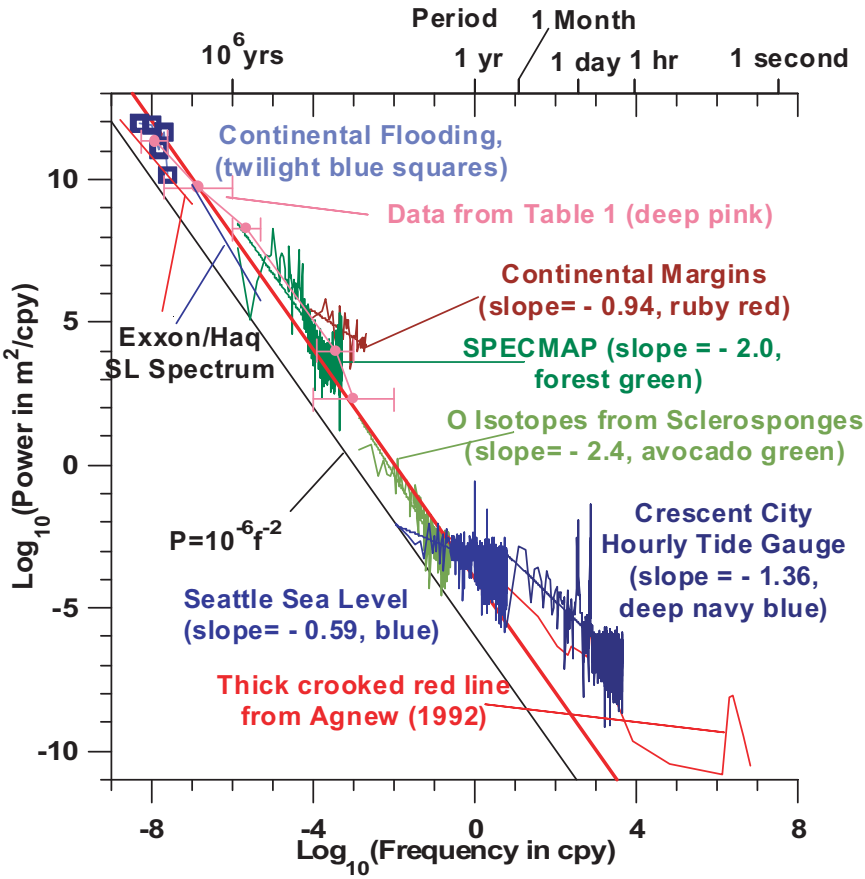

Figure 1. Power spectrum of sea level change. The five pink points and connecting line at the lowest frequencies are from Table 1 and are shown with horizontal bars indicated the frequency ranges of the signals. The information in the topmost of these data points has been reanalyzed and the average spectrum derived from six continental flooding estimates is shown by the five twilight blue squares. The two thick red and blue lines at the top left of the graph show the spectra (described more fully in Figure 3) for the Exxon/Haq sea level curve (Figure 2). The wiggly forest green line plus its best fitting straight line (shown separately in Figure 4) between periods of ~780 ka and 2000 years is a sea level signal calculated from the SPECMAP time series by assuming that the oxygen isotopic variation from the present day to the last glacial maximum was equivalent to a sea level change of 120 m. Spectral peaks can be seen at 100, 41, 23, and 19 ka, representing Milankovitch signals. There is also a broad prominent peak at 60 ka. The shorter ruby red line plus its best fitting straight line between periods of 12 ka and 500 years is from seismic records of a sedimentary sequence observed over a continental margin. The Seattle sea level curve spectrum from monthly mean tide gauge records, representing periods between 94 years and 2 months is shown, with its best fitting line, in blue. An annual and a semi-annual peak can be seen, but there is no sign of the 14-month pole tide. An hourly tide gauge record for Crescent City (of length 59 days) plus its best fitting line is shown in deep navy blue, representing periods between 6.2 and 4383 cpy. The double peak at the lower frequency shows the luni-solar and principal solar diurnal tides. The triple peak at the higher frequency shows the principal lunar and solar, and the larger lunar elliptical semidiurnal tides. The thick red line at the highest frequencies is from *Agnew* [1992] and shows the power in ocean waves with a peak at a period of ~10 s and a symbolic peak at the semidiurnal tidal period. The line from Agnew lies directly over the spectrum for the Seattle tide gauge record. There is also the power spectrum from a record of oxygen isotopes in sclerosponges, which has been shifted vertically so that its power level is consistent with the data at lower and higher frequencies, plus its best fitting line, in avocado green. The red straight line running diagonally through the graph is a line with a slope of $-1/f^2$ (i.e., $\log(P) = -4 - 2\log(f)$ or $p = 10^{-4}/f^2$), for the sake of comparison. The thin black line is parallel to and offset from this line by 2 orders of magnitude in power.

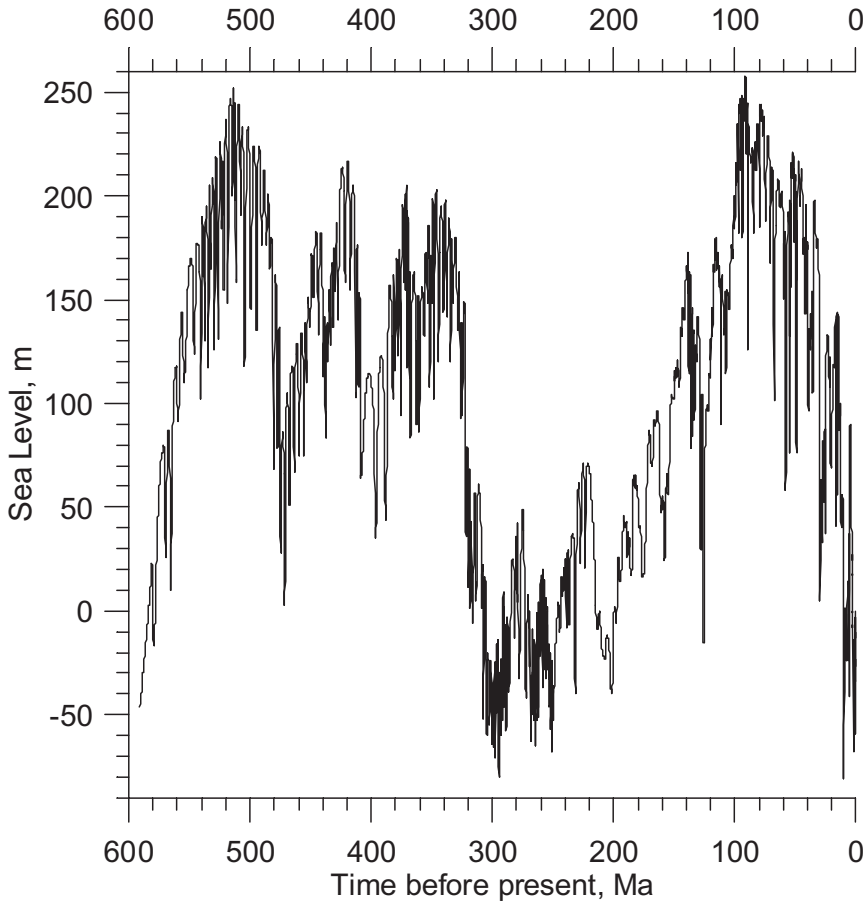

Figure 2. The Exxon/Haq sea level curve for the past 591 Ma. The data points are spaced every 0.1 Ma. Times of low sea level (except for today) are thought to be correlated with supercontinent formation such as Pangea at ~300 mybp and Pannotia or Rodinia in the pre-Cambrian.

made at a frequency of 0.1 cpmy. This plot uses a timescale of Ma rather than the 1 year scale of Figure 1. After transforming the units, the red and blue lines are also plotted on Figure 1 in the upper left-hand corner. The agreement with the other data is quite good, especially when it is realized that the Exxon/Haq sea level curve is supposed to be eustatic, having had epeirogenic continental movements removed. Therefore it would be expected to have somewhat lower power than the other records at the low frequency end, which come from relative sea level measurements. However, some people [e.g., *Sloss*, 1991] believe that there is still a large tectonic component in this sea level curve. The sea level record was divided into four equal segments and the average power from the segments was calculated to see if there was any sign of a periodicity with significantly enhanced power over the average. The average spectrum below a frequency of 0.2 cpmy was extremely smooth. There was, however, some slight indication of enhanced power at a frequency of 1 cpmy, which can also be detected in the signal spectrum shown in Figure 3.

[12] The other spectrum which overlaps this result from the continental margins comes from a completely different data set, the SPECMAP record of oxygen isotopes derived from pelagic foraminifera [*Imbrie et al.*, 1984]. This spectrum is shown separately in Figure 4 as well as on Figure 1. The SPECMAP data consist of oxygen isotopic compositions of pelagic foraminifera, expressed in units of standard deviation, since the record is a stacked compilation from a number of different cores and the data from the cores were compared by normal-

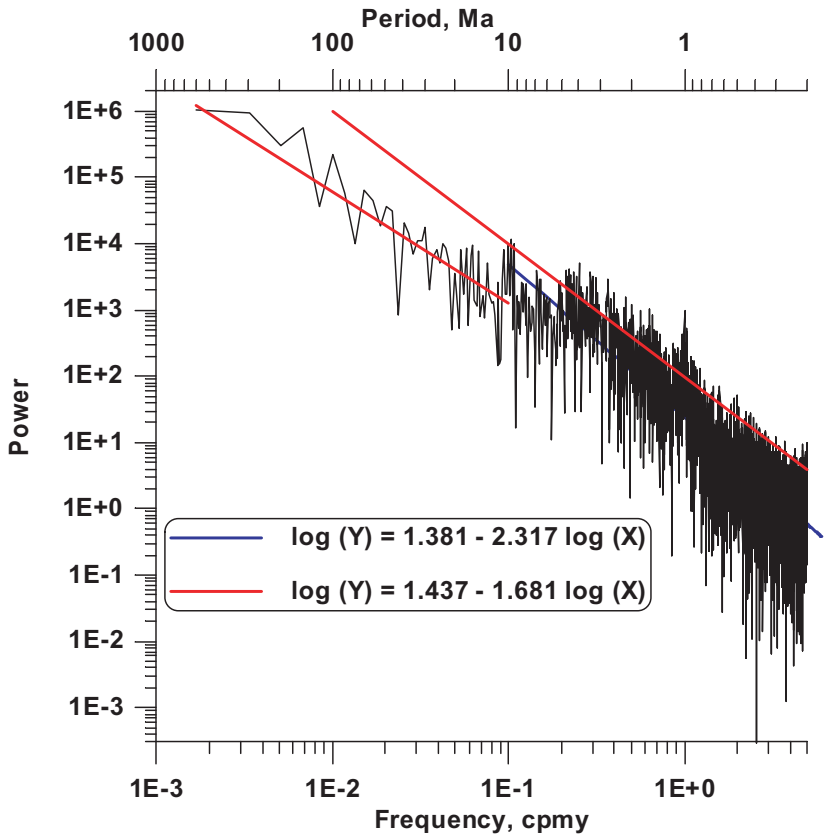

Figure 3. Power spectrum of Exxon/Haq sea level curve (Figure 2). Maximum period is 591 Ma, and minimum period is 0.2 Ma. The equations of the two straight red and blue lines drawn through the data are shown. The separation between the data used to calculate these lines is at a frequency of 0.1/Ma. The abscissa has units of cycles per million years, and the ordinate has units of meters^2 per cycle per million years.

izing by the standard deviations of the oxygen isotopic variation in each individual core. The SPECMAP time series has a data point every 1000 years for the past 782,000 years. The spectral index of the whole spectrum is close to −2.0, and the largest peak to be seen at the low frequency end of the spectrum has a period of 98 ka, representing the response of Earth to the Milankovitch periodicity associated with orbital eccentricity variations or another of the several mechanisms that have been advanced to explain this periodicity [e.g., *Muller and MacDonald*, 1997]. Peaks at 41, 23, and 19 ka represent the other major peaks predicted by the Milankovitch theory, and there is another strong and broad peak at a period of 60 ka that may be related to the weak 58 ka eccentricity signal of the Milankovitch theory. In order to obtain a sea level record from the oxygen isotope record, it was assumed that sea level is linearly related to the oxygen isotopic composition of the foraminifera, which can either reflect ocean surface temperature or the changing isotopic composition of sea water due to waxing and waning of continental ice sheets, or some combination of these two end member models. The coefficient that relates the oxygen isotopic signal to sea level is the observed change in sea level on going from the present day to the last glacial maximum, when sea level was 120 m lower than today [*Bard et al.*, 1990]. No assumption has been made about how much of the oxygen isotopic signal (which in any case is expressed in terms of standard deviation and not per mil variations) is caused by temperature and how much by ice storage of isotopically light fresh water. The sea level change between the last glacial maximum and today is established independently of the oxygen isotopic variations. The flattening of the spectrum at high frequencies (Figure 4) may be due to white

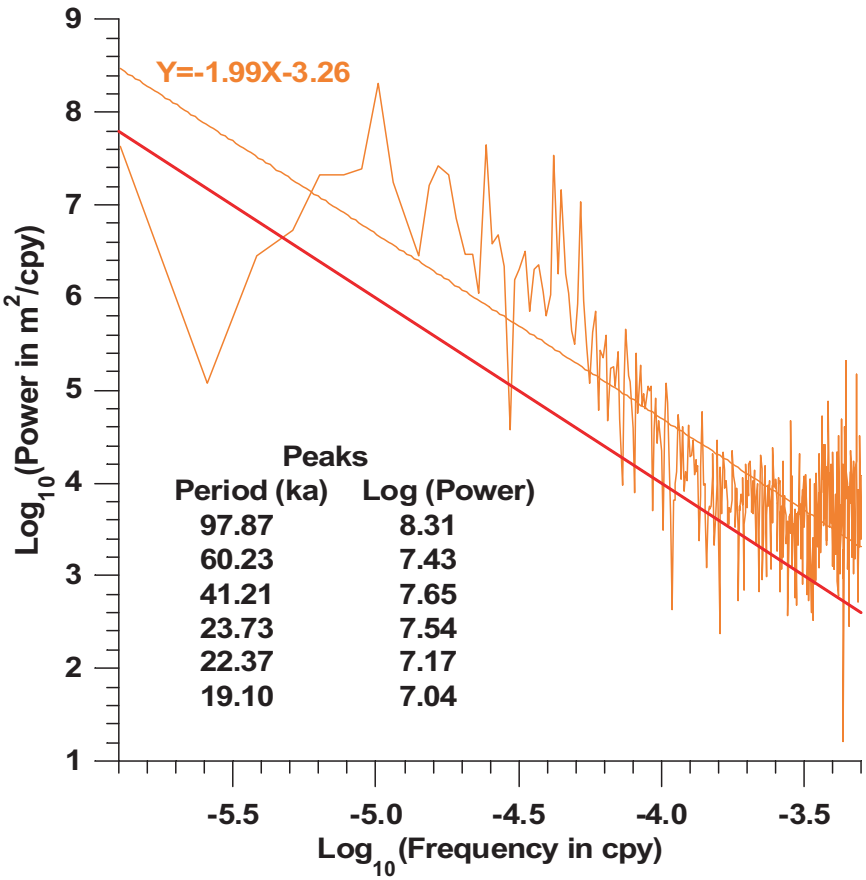

Figure 4. Power spectrum of the SPECMAP time series (detail from Figure 1). The six strongest peaks (neglecting the fundamental) are identified. The sea level signal was established by assuming that the latest change in oxygen isotopes (on going from the last ice age to the present interglacial) was equivalent to a sea level change of 120 m.

noise entering the signal, a likely event because the power at the high frequency end of the spectrum is very low compared with the 98 ka signal.

[13] Aliasing can always present problems when performing Fourier analysis on finite records of discrete time series. However, this problem is not severe if the natural spectrum has a large negative slope [*Wunsch*, 1972]. Figure 5, derived from formulae by *Wunsch* [1972], shows the change that can be produced in a power spectrum due to aliasing. The original spectrum, shown as a straight line, is a spectrum in which the power falls off as $1/f^2$. The data separation period is normalized at 1, giving a Nyquist period of 2 (frequencies of 1 and 0.5, respectively). The aliased spectrum is shown as a curved line. The maximum difference is seen at the Nyquist frequency, where the aliased power is about a factor of 2.5 greater than the original power. If the number of data used is greater than 50, then the straight line slope through the aliased power spectrum is less than -1.85 (i.e., close to -2).

[14] At shorter periods (between 500 and 100 years), there is still a paucity of available data. However, at ~100 years or so, information from tide gauges becomes available. In order to quantify better the tide gauge information, I have used data from Seattle, which consist of monthly mean sea level measurements, taken over a time interval of 94 years, to add to Figure 1. This then gives an estimate of the spectrum between periods of 2 months and 94 years. The power spectrum for the Seattle tide gauge data lies directly over the spectrum presented by *Agnew* [1992] for the appropri-

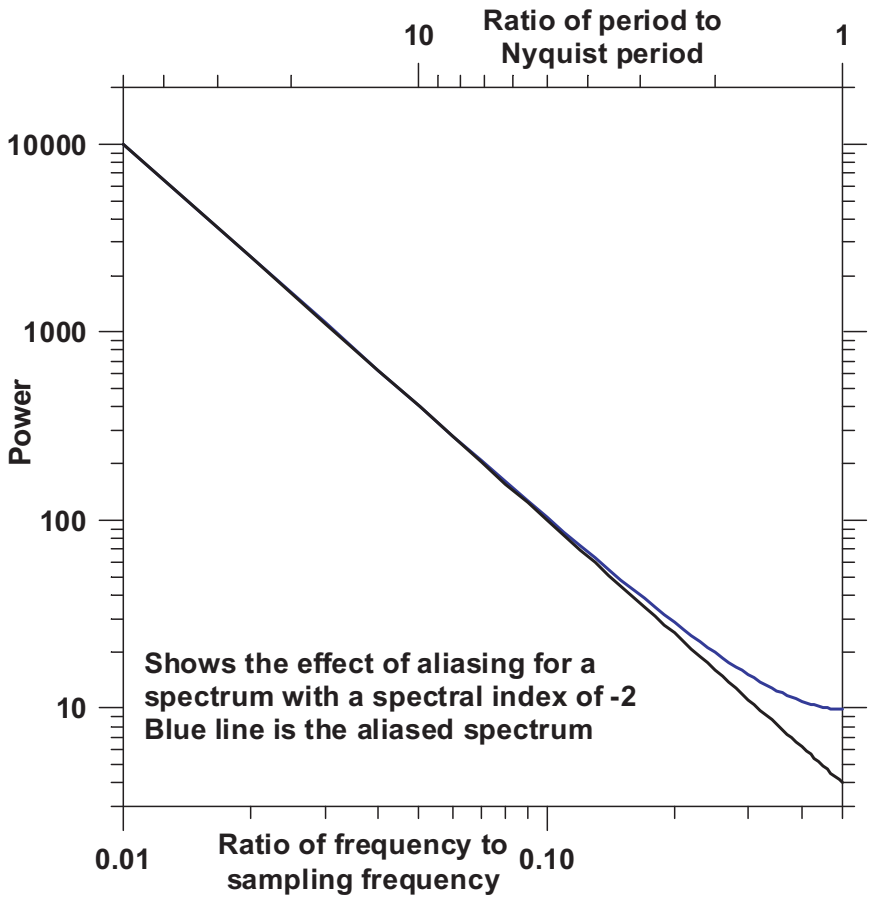

Figure 5. Power spectrum showing aliasing effect [*Wunsch*, 1972]. The sampling frequency is 1, and the Nyquist frequency is 0.5 (periods are 1 and 2). Fifty frequencies are plotted going from 0.01 to 0.5. The random walk $1/f^2$ spectrum is shown by the straight line, and the aliased spectrum is shown by the blue line. Provided that the length of the record is much longer than the sampling period (i.e., many samples), aliasing does not have much effect. Maximum effect is at the Nyquist frequency where the aliased power is ~2.5 times the original power. At half the Nyquist frequency the aliased power is only ~20% larger than the real power.

ate periods (see Figure 1). In the spectrum an annual and a semi-annual term are easily recognizable. The pole tide does not produce a signal that is distinguishable from the background. Some numerical results from other long monthly mean tide gauge records are shown in Table 2. As can be seen, many of the tide gauge spectra have spectral indices close to −0.5. Aliasing is unlikely to produce a significant change in the slopes of the power spectra for these records because the data are monthly mean data that have averaged out almost all of the variation with periods less than one month. Part of the variance difference between different tide gauge records may be due to the differing record lengths. For instance Cuxhaven and Den Helder are the two longest records and have the greatest and third greatest variances. Long records such as these will sample lower frequencies that have greater power. Part of the variance difference is undoubtedly due also to the geographic location of the stations.

Table 2. Power Spectrum of Monthly Tide Gauge Records

Location	Record Length, Years	Total Variance, m^2	Spectral Index
Boston	72	0.237	−0.59
Brest	83	0.575	−0.44
Cuxhaven	144	2.042	−0.17
Den Helder	130	0.877	−0.16
Dublin	57	1.023	−0.38
Honolulu	88	0.254	−0.14[a]
Key West	80	0.203	−0.63
Seattle	94	0.409	−0.59
Sydney	97	0.270	−0.56

[a]Also a slope of −1.27 at higher frequency.

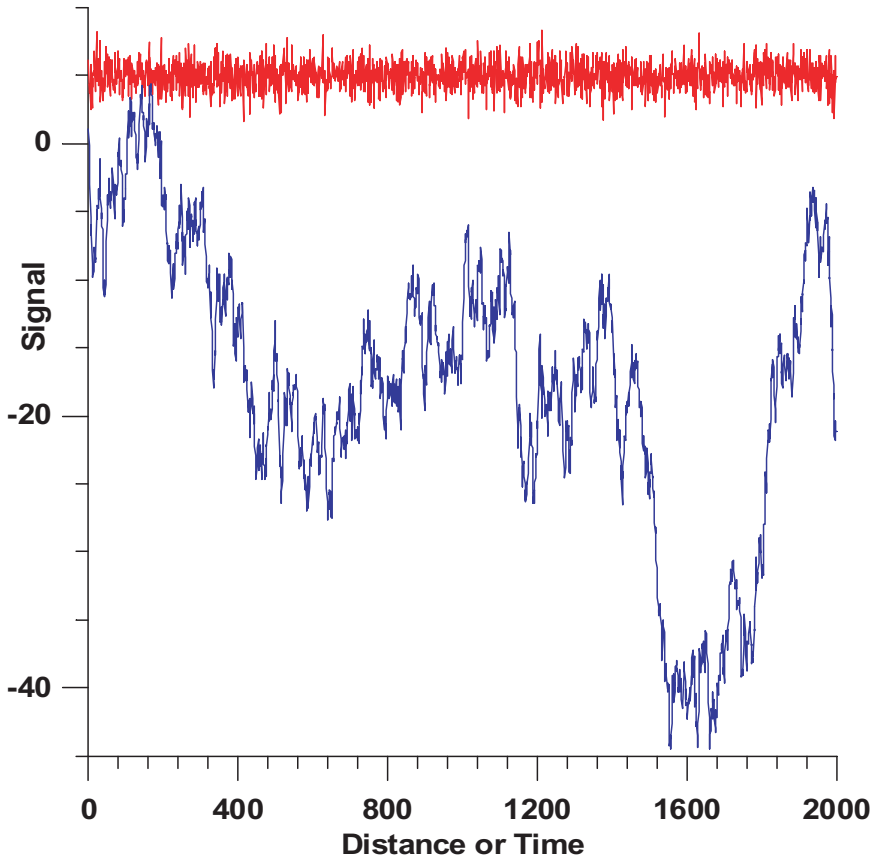

Figure 6. Red top curve. A set of 2000 normally distributed numbers with zero mean and unit standard deviation displaced five ordinate units upward (a white noise signal). Blue bottom curve. The serial sum of the top numbers (a random walk signal).

[15] At the high frequency end of the scale, the results from *Agnew* [1992] have been added. The original spectrum has been lost, but the one presented in Figure 1 is the dashed approximation shown by *Agnew* [1992] in his Figure 6. The tidal components are not all present, but the largest, the semi-diurnal tide, is represented by the symbolic peak at the appropriate frequency. This peak is not as large as the one shown in Agnew's original spectrum. The broad peak between periods of 1 min and 1 s is caused by wave motion.

[16] Also shown in Figure 1 is an example of a sea level spectrum from a tide gauge where the normal tidal signals are present. This is the hourly tide gauge record from Crescent City, of length 59 days. This spectrum, if expanded in scale, clearly shows two separate diurnal tides and three separate semi-diurnal tides. It has a slope considerably less than -1 and lies above the generalized spectrum of *Agnew* [1992]. Other hourly tide gauge records show large variations in power level for this portion of the spectrum so that the discrepancy between the spectrum of Agnew and that given by the Crescent City data just indicates this variation from one place to another. Aliasing is also not likely to be a problem with these records, which are composed of hourly mean data, therefore having averaged out periods smaller than an hour. The practice of using stilling wells also damps out short period variations from tide gauge records, especially those from waves.

[17] Also plotted on Figure 1 is the data set of oxygen isotopic composition of sclerosponges [*Swart et al.*, 1998, 2002], kindly given to me by Peter Swart. The data are for the ^{18}O composition of sponges every other year or so going back to 1266. There are 350 data between 1266 and 1989 giving an average data span of 2.1 years. The spectral index

of the power spectrum from this data set is close to −2. The level of the sea level signal was adjusted so that the spectrum fit in with spectra on either side. If the sea level variation is assumed to be similar to that seen over longer periods, in which a 2 per mil change in the ^{18}O composition is equivalent to 120 m, the level of the spectrum is far too great. In order to get the spectrum in its position as shown in Figure 1 the signal then had to be divided by 100. The main reason for showing the sclerosponge data is to demonstrate that at least one signal which is climatically controlled has a spectral index of −2 in the region of the gap in true sea level data.

[18] Although there is still a gap in the power spectrum, it has been closed significantly by use of sedimentary sequence data and by information on sea surface oxygen isotopic composition. These two new data sets, despite coming from completely different data types, agree very well in their overall estimate of the signal power at the overlapping

Table 3. Power Spectrum Slope According to Different Treatments

Data Window[a]	Best Fitting Line Removed from Data	Frequency Distribution	Slope
Box Car	No	Uniform Log	−1.80
Parzen	No	Uniform Log	−1.82
Hanning	No	Uniform Log	−1.81
Welch	No	Uniform Log	−1.87
Box Car	No	Uniform Freq.	−1.77
Box Car[b]	Yes	Uniform Log	−1.61
Box Car[b]	Yes	Uniform Log	−1.99

[a] *Press et al.* [1986].
[b] Removing a best fitting line before obtaining spectrum severely reduces fundamental power. The last result omits fundamental power and last two results are shown in Figure 7.

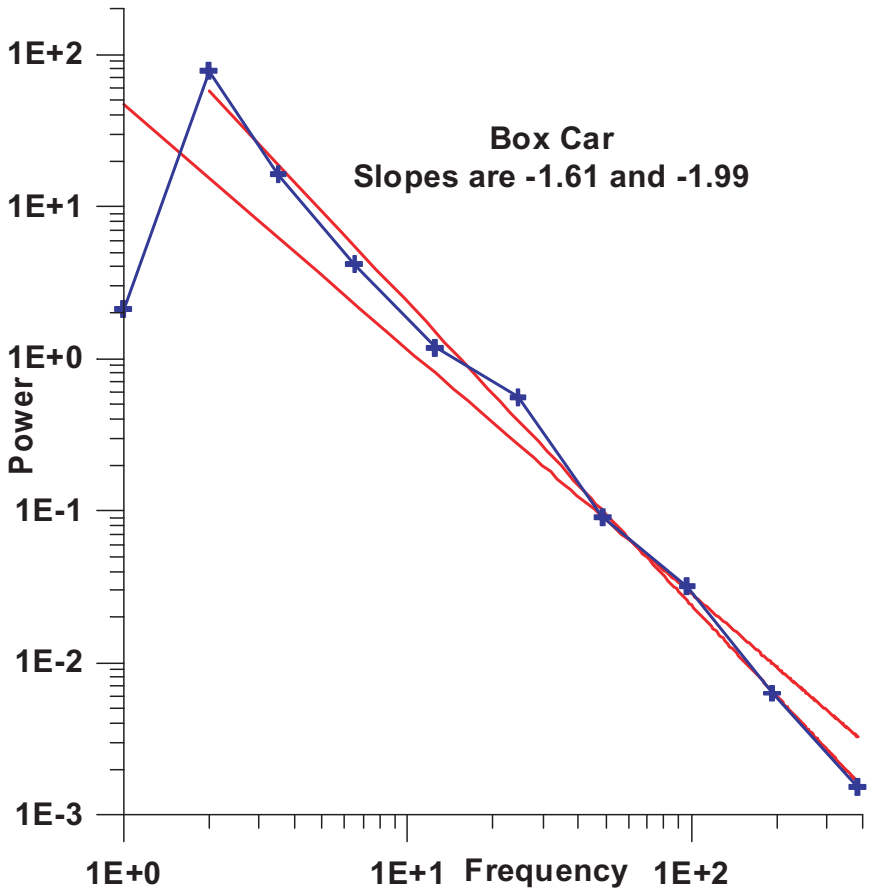

Figure 7. Power spectra from Table 3, using the random walk signal shown in Figure 6. Powers for various harmonic ranges are averaged and are plotted at the average harmonic value within each range. The left-hand point is for the fundamental (harmonic 1), the second point is for harmonic 2, the third point is for harmonics 3 to 4, the fourth point is for harmonics 5 to 8 etc. The red lines are best fitting lines through all points, and all but the fundamental, which has low power because a best fitting line was removed from the signal before taking the spectrum.

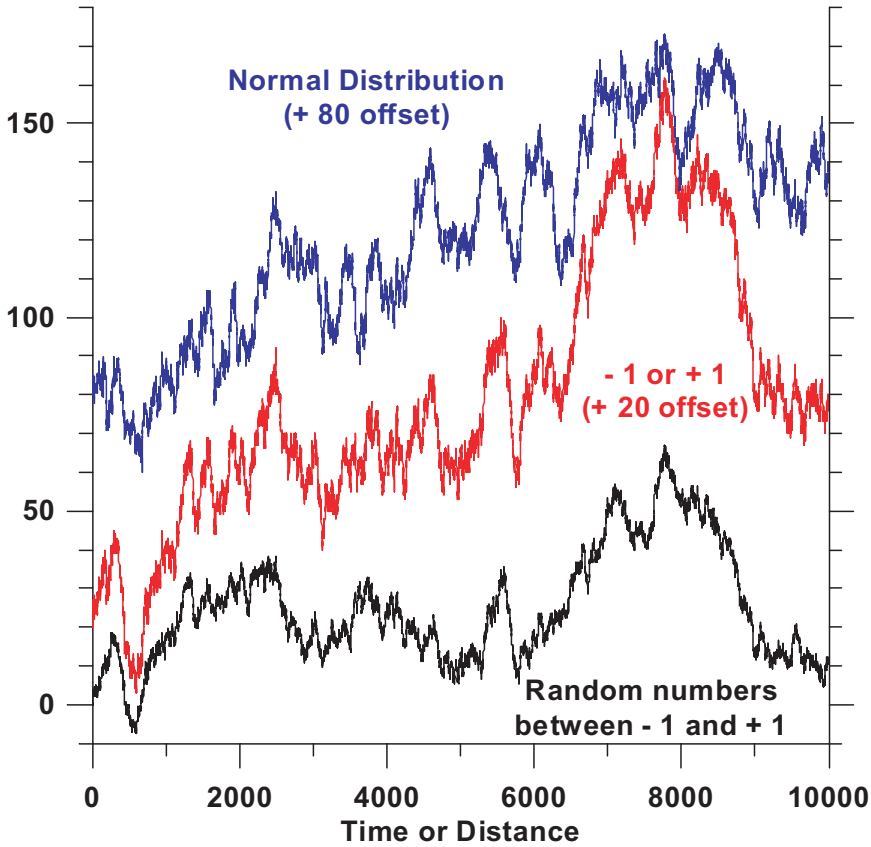

Figure 8. Random walk signals. The black bottom line was generated from random numbers uniformly distributed between −1 and +1. The middle red line (displaced 20 ordinate units for clarity) was generated from digits −1 and +1 chosen according to the sign of the numbers used to generate the bottom curve. The top blue curve (displaced 80 ordinate units for clarity) was generated from the same numbers used to generate the bottom curve but reorganized into a zero mean unit standard deviation normal distribution.

frequencies. It is a remarkable fact that the sea level spectrum resembles a $1/f^2$ spectrum throughout a range of frequencies of ∼12 decades, apart from the 0.2–100 a periods recorded by tide gauges.

3. Random Walk Spectra

[19] A spectrum that has a spectral index of −2 is equivalent to the spectrum of a signal generated by a random walk process. *Wunsch* [1992] has discussed some of the implications of a time series that has a spectral index of −2. If a record of a certain length is available (for instance, the temperature at a land station) then some information is available about fluctuations that are shorter or equal in time to the length of the signal. If the signal is increased in length (because more years of data are added at the end), then if the signal has a $1/f^2$ slope, longer period signals will become observable, and since these signals have greater amplitudes, they will produce a variation which has not been seen before. It is then very easy for scientists to point to this variation and state that some new phenomenon (anthropogenic?) must have caused the new signal. In reality, it may just be normal processes causing the signal to vary, in ways similar to a random walk signal.

[20] As an example, Figure 6 shows a random walk signal generated using a random number generator. The top curve shows a white noise signal generated using a set of 2000 random numbers drawn from a Gaussian distribution with zero mean and unit standard deviation. The lower curve shows the result of serially summing these numbers to get a random walk signal. The top curve has been displaced upward five ordinate units for clarity. The power spectrum of the white noise has a slope not

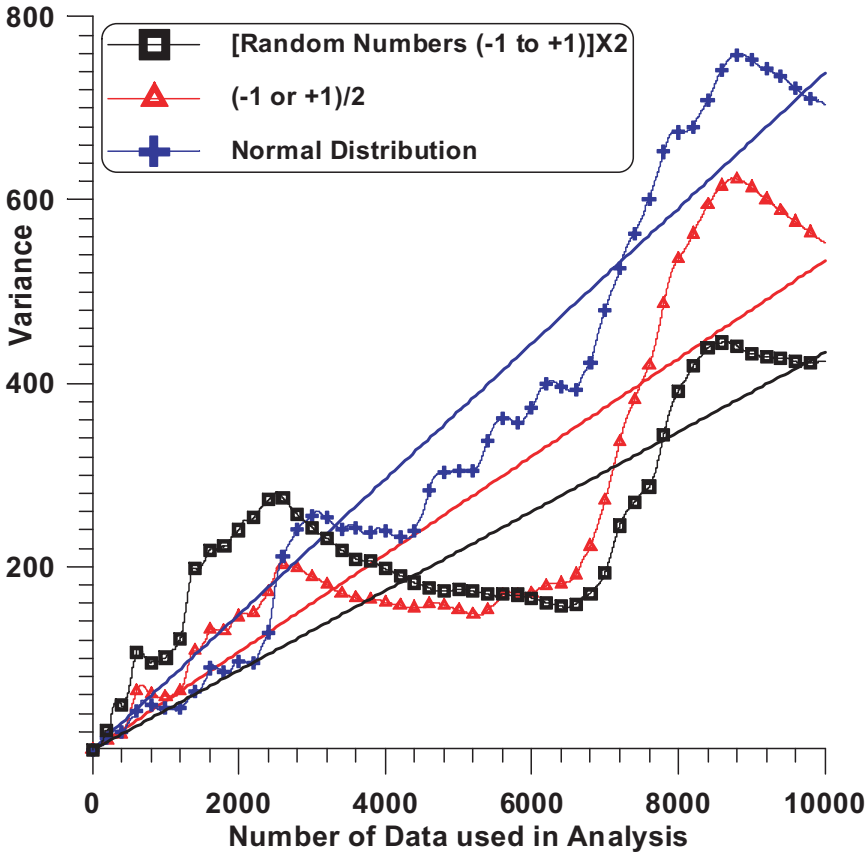

Figure 9. True variance of signal according to the number of data used to generate the signal. The signals are shown in Figure 6. The variance of the signal generated by −1 or +1 has been divided by 2, and the variance of the signal generated by uniform numbers between −1 and +1 has been multiplied by 2 for comparison purposes. Best-fit straight lines running through the origin are also shown.

significantly different from zero. The slope of the power spectrum of the random walk signal is close to −2. The difference in slope between using a boxcar, Hanning, Welch, and Parzen data window is insignificant. Table 3 gives some results. Those results marked with a "Uniform Log" frequency distribution are done by obtaining average power for approximately equal ranges of log(frequency). The first and second numbers are for the fundamental and second harmonic. The third number is the average of the third and fourth harmonics plotted at frequency 3.5, the next is the average of the fifth to eighth harmonics plotted at a frequency of 6.5 etc. The uniform frequency result is obtained by weighting all frequencies uniformly. The results of the last two calculations in Table 3 are shown in Figure 7.

[21] Another way of looking at this phenomenon is to realize that the variance of a random walk spectrum is linearly related to the length of the record [*Agnew*, 1992; *Wunsch*, 1992].

$$v_n = v_w n. \tag{1}$$

In this equation v_n is the variance of the random walk signal which lasts n steps, and v_w is the variance of the white noise which when summed gives the random walk signal. The mean square value of the wander between one observation and another one separated from it by a constant value of time or distance is also dependent linearly on the separation between the two measurements [*Agnew*, 1992]. Equation (1) shows that as the record becomes longer, the data must go into new territory, so as to increase the variance of the whole record.

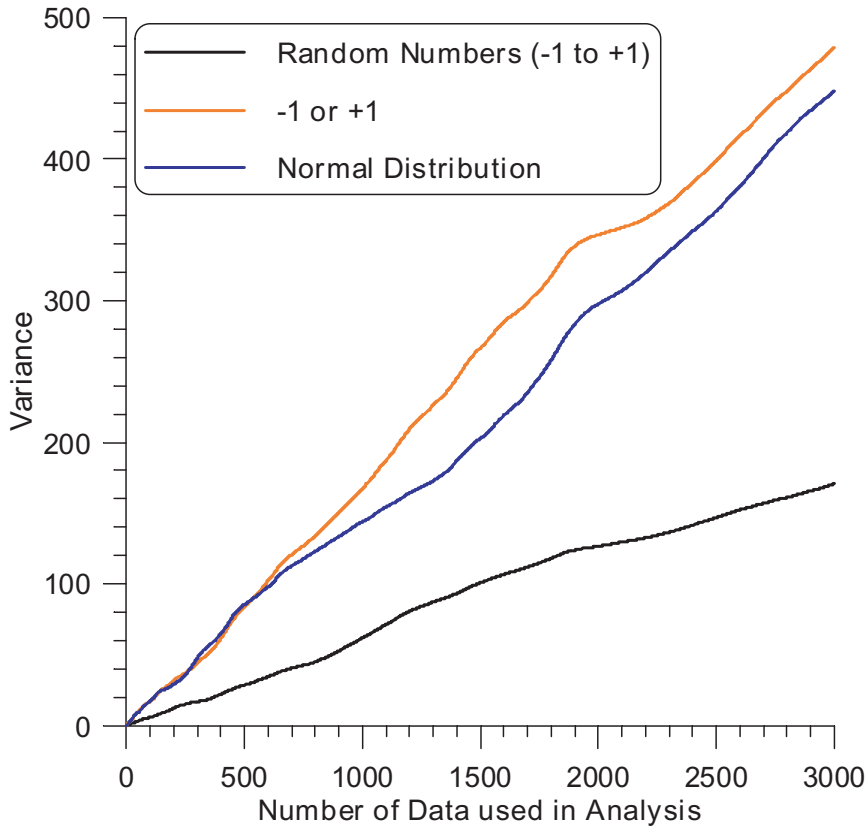

Figure 10. True variance of signal according to number of data used to generate the signal. This is the average of 40 different renditions and shows very smooth increase of variance with record length, compared with Figure 9.

Figure 8 shows three random walk signals of 10,000 steps generated from the same set of random numbers. For one signal the random numbers were randomly distributed between −1 and +1. For the next signal, the numbers were either −1 or +1, depending on the sign of the original set. For the third signal the numbers were transformed into a set of zero mean unit standard deviation random numbers. The variance for each random number signal is shown in Figure 9, indicating a general but not very consistent rise in variance as the signal length increases. If many different random walk signals are calculated and the variance for all records of the same length is averaged, the rise of variance as a function of record length is much more consistent (Figure 10).

[22] In Figure 1 there is still a gap in information at periods greater than those recorded by tide gauges (i.e., ∼100 years). However, judging from the considerable array of data through other spectral ranges shown in Figure 1, it seems likely that there will be sources of sea level variation which start to manifest themselves at periods greater than 100 years, and the slope of spectrum of these sea level variations is likely to have a spectral index of about −2, so that this portion of the spectrum will join onto that seen in the SPECMAP data. Should such a situation arise, then sudden changes in the rate of sea level change may easily be caused by natural phenomena, without having to call on special processes, such as anthropogenic global warming. Nonanthropogenic global temperature change, being a natural phenomenon, could be a perfectly viable cause of sea level change.

4. Discussion

[23] The best-fitting curve through the data shown in Figure 1 has the form

$$P = 10^{-4} f^{-2}, \tag{2}$$

where P is the power in m^2/cpy and f is in cpy. There are several spectrally narrow causes for some

of the sea level variation shown in Figure 1. For instance tidal variations have specific periods. Also, the Milankovitch theory of ice ages predicts that the sea level variations caused by these ice ages should have specific frequencies, which can be seen in the tuned SPECMAP time series. Various nonperiodic oceanographic parameters such as intensity changes of geostrophic currents can also cause sea level changes toward the high frequency end of the scale shown in Figure 1. Atmospheric effects are also important nonperiodic forcings at the high frequency end of the scale. At the low frequency end of the timescale, many factors may contribute, including ridge crest volume, ice volume, hot spot activity that can cause both eustatic and epeirogenic effects, changes in continental and oceanic area due to continental collisions and continental breakup, ocean water temperature changes and sediment volume effects [*Harrison*, 1988, 1999]. Most of these are internally generated factors. However, because of the regular nature of the spectrum, excluding the peaks at specific frequencies whose causes are usually known, there may be a more general cause for the distributed spectrum at the low frequency end. Changes in dynamic topography, caused by variations in asthenospheric convection current patterns, can cause surface topography changes resulting in sea level variations [*Lithgow-Bertelloni and Gurnis*, 1997; *Gurnis*, 2001]. Another cause of epeirogenic vertical movement may be temperature changes at the base of the lithosphere [*Harrison*, 1988]. These will cause the lithosphere to change its temperature, resulting in expansion or contraction of lithospheric thickness, and a change in the position of the lithospheric surface. In this section, I discuss this as a possible cause for some of the sea level changes and investigate the temperature changes necessary to give the observed slope to the sea level power spectrum, without implying that this is the only phenomenon causing these sea level changes.

[24] For one-dimensional heat flow and no heat sources, the diffusion equation is

$$\frac{\partial^2 T}{\partial z^2} = \frac{1}{\kappa}\frac{\partial T}{\partial t}, \tag{3}$$

where T is the temperature, t is the time, κ is the thermal diffusivity, and z is the distance upward from the bottom of the lithosphere. A solution that has sinusoidally varying temperature at the bottom of the lithosphere is given by the following equations.

$$T = T_0 \exp(-kz)\cos(\omega t - kz), \tag{4}$$

where

$$\omega = \frac{2\pi f}{3.16 \times 10^7} \tag{5}$$

and

$$k = \sqrt{\frac{\omega}{2\kappa}}. \tag{6}$$

[25] In these equations, T_0 is the amplitude of the temperature signal at the bottom of the lithosphere, ω is the angular frequency (s^{-1}), k is the wavenumber of the vertical variation of temperature within the lithosphere (m^{-1}), and f is the frequency in cpy [*Garland*, 1979]. The thermal expansion of the lithosphere is then given by

$$\Delta z = \int_0^L \alpha T dz, \tag{7}$$

where L is the lithospheric thickness and α is the volume coefficient of thermal expansion. Provided that $L \gg 1/k$, which given a lithospheric thickness of 125 km means a period $t \ll 2000$ Ma, the approximate solution to equation (7), putting $L = \infty$, is

$$\Delta z = \frac{\alpha T_0}{2k}(\sin \omega t + \cos \omega t). \tag{8}$$

The amplitude of the elevation change is therefore equal to

$$A_z = \frac{\alpha T_0}{\sqrt{2}k}. \tag{9}$$

For a thermal diffusivity of $8.3 \times 10^{-7} m^2 s^{-1}$ and a volume thermal expansion coefficient of 3.35×10^{-5} °K^{-1}, the power of the elevation change ($0.5A_z^2$) is

$$P_{A_z} = \frac{2.342 \times 10^{-9} T_0^2}{f} \tag{10}$$

This can then be equated with equation (2) and integrated over any frequency range to determine the total temperature variation.

$$P_{T_0} = \frac{42700}{f} {}^{\circ}\mathrm{K}^2 \tag{11}$$

$${}_{f_1}T_{f_2} = \sqrt{\left(42700 \log_e \frac{f_2}{f_1}\right)} {}^{\circ}\mathrm{K}. \tag{12}$$

In equation 11, P_{T_0} is the power in the temperature signal as a function of frequency f. The temperature therefore has a spectral index of -1 and is similar to flicker noise [*Mao et al.*, 1999]. In equation (12) the expression is for the rms temperature signal from frequency f_1 to f_2. Thus even over three decades of frequency, the signal is only $\sim 540^{\circ}$K. Other sources of relative sea level change will reduce this number. For instance, the tidal and ice age signals, as well as the other causes mentioned above, will reduce the magnitude of this temperature signal. At very long periods it seems likely that epeirogenic motions are caused by dynamic topographic changes [*Gurnis*, 1993; *Hager et al.*, 1985]. However, there are postulated to be significant temperature changes which could occur at the bottom of the lithosphere [*Gurnis*, 1988; *Glatzmaier and Schubert*, 1993], and these could be some of the driving influences on the relative sea level power spectrum discussed in this paper. In some of the models of *Glatzmaier and Schubert* [1993] the temperature variations at a relative radius of 0.95 appear to be plus or minus several hundred degrees Kelvin, so the 540°K number quoted above seems reasonable.

[26] *Hsui et al.* [1993] have discussed fractal analyses and power spectra of several sea level change signals. They used mostly the Hurst index, which is related to the spectral index by the equation $\beta = 2H_u - 1$, where $-\beta$ is the spectral index and H_u is the Hurst index [*Turcotte*, 1997, equation 7.61]. However, Turcotte has shown that this equation is only useful for a small range of the Hurst index. In particular, when β is greater than ~ 0.85, the Hurst index starts to saturate and does not grow much above 1 even for β values of 3. For four of the data sets analyzed by Hsui et al., the Hurst indices were close to 1, and so it is not possible to determine accurately the spectral index of these four records by using the Hurst index in Hsui et al. However, one record, which had a Hurst index of 0.92, was also analyzed spectrally, giving a β value of 1.5, considerably greater than the value that is calculated using the equation (0.84). This record was ostensibly a 30 Ma record of sea level developed from sedimentary sequences published by *Haq et al.* [1988], but the power spectrum given in the paper showed a record length of 15 Ma and a Nyquist period of 500 ka.

[27] *Gauthier* [1999] has produced power spectra for several different types of climatic proxy records. A tree ring growth index spectrum for an 8000-year record showed an almost white spectrum (but note that more recent analyses have shown different behavior). Oxygen isotopic records from an ice core (periods between 350 years to 250 ka) show a spectrum with a spectral index of about -1.1, which may be on the shallow side if aliasing has taken place. Results from the Devils Hole calcite (periods between 3 ka and 500 ka) showed a spectral index of about -2.1.

[28] *Courtillot and Le Mouël* [1988] have produced a schematic power spectrum for the geomagnetic field that extends over 12 decades of frequency, with periods ranging from 36 s to 30,000 years. This spectrum is also generally a $1/f^2$ spectrum. Just as in the sea level spectrum, there are many different causes for the geomagnetic field spectrum. At the high frequency end, the causes are usually external to the Earth, whereas at the low frequency end, internal phenomena such as polar wander, continental drift, reversals and secular variation, are more important.

[29] *Avnir et al.* [1997] surveyed seven years of the *Physical Review* and *Physical Review Letters* and found 95 studies in which the logarithm of power was linearly related to the logarithm of frequency or wave number. The maximum frequency range was between 2.7 and 3 decades for the two studies that showed the greatest frequency range. *Radlinski et al.* [1999] have presented neutron and X-ray scattering data showing that rocks are fractal in nature over at least 3 orders of magnitude, implying that this is close to the maximum limit likely to be observed.

For a power spectrum with a spectral index of −2, the fractal dimension is 1.5 [*Turcotte*, 1997].

[30] This paper has shown that sea level is approximately fractal over 12 orders of magnitude. I await claims of fractal nature over more decades than this!

5. Conclusions

[31] Sea level change has been studied by determining the Fourier power spectra of various different types of record. The periods examined ranged from 591 Ma down to 5 s, a range of ∼15.5 orders of magnitude. At the long period end of the record, results were obtained from sea level curves derived from continental margin sedimentary cycles, flooding estimates of continents by marine waters, the SPECMAP oxygen isotope signal transferred to sea level variations estimates, and some other observations. At the short period end of the scale, results were obtained from tide gauges and from previously published water pressure measurements. Over much of this range of periods, the spectrum had a spectral index of about −2 and is therefore equivalent to a spectrum produced by a random walk phenomenon. In particular there is a $1/f^2$ variation between periods of about 600 Ma and 100 a (the slope of log(power) versus log(frequency) = −2). Here the spectrum flattens out and varies by $1/\sqrt{f}$ for about two decades of period, down to about a period of a year. Here the spectrum again slopes down with a slope considerably less than −1 until it flattens out again at a period of about an hour, where wave action becomes the dominant cause of sea level variation, creating a peak in the spectrum at a period of ∼10 s. Many different phenomena can affect sea level over such a wide range of period, such as epeirogenic motions of the continents, secular changes in ocean basin volume produced by sea floor spreading, continental collision, and other effects. Over shorter periods ice age periodicities suggested by the Milankovitch theory of ice ages is an obvious cause, as well as aperiodic causes such as ocean currents. At shorter timescales yet, tidal effects are important, and waves become dominant at the shortest periods. One possible cause of epeirogenic change examined in greater detail was the effect caused by heating and cooling of the bottom of the continental lithosphere by the variable temperature within the asthenosphere below it. Temperature changes necessary to produce the observed signal of relative sea level change appear to be reasonable. Signals similar to those studied in this paper frequently do surprising things when longer records are obtained. As the record length becomes longer, signals of greater period, with much larger amplitudes, start to become important. This means that it is difficult or impossible to judge whether a specific signal variation not seen before in a shorter record is part of the natural variation or whether it may be a new type of signal produced by human activity.

Acknowledgments

[32] I thank Peter Swart for giving me the isotopic data on sclerosponges, Tim Dixon for commenting on the manuscript, and Duncan Agnew for sending me his summary power spectrum of sea level change. I thank Carl Wunsch for a constructive review that materially improved the paper. Conversation with David Chapman was illuminating.

References

Agnew, D. C., The time-domain behavior of power-law noises, *Geophys. Res. Lett.*, *19*, 333–336, 1992.

Avnir, D., O. Bilham, D. Lidar, and O. Malcai, Is the geometry of nature fractal?, *Science*, *279*, 39–40, 1997.

Baltuck, M., J. Dickey, T. Dixon, and C. G. A. Harrison, New approaches raise questions about future sea level change, *Eos Trans. AGU*, *77*, 385, 1996.

Bard, E., B. Hamelin, R. G. Fairbanks, and A. Zindler, Calibration of the ^{14}C time scale over the past 30,000 years using mass spectrometric U-Th ages from Barbados corals, *Nature*, *345*, 405–409, 1990.

Barron, E. J., C. G. A. Harrison, and W. W. Hay, Paleogeography, 180 million years ago to the present, *Eclogae Geol. Helv.*, *74*, 443–470, 1981.

Bond, G. C., Evidence for some uplifts of large magnitude in continental platforms, *Tectonophysics*, *61*, 285–305, 1979.

Church, J. A., et al., Changes in Sea Level, in *Climate Change 2001. The Scientific Basis: Contribution of Working Group I to the Third Assessment Report of the Intergovernmental Panel on Climate Change*, edited by J. T. Houghton et al., pp. 639–693, Cambridge Univ. Press, New York, 2001.

Courtillot, V., and J. L. Le Mouël, Time variations of the Earth's magnetic field: From daily to secular, *Annu. Rev. Earth Planet. Sci.*, *16*, 389–476, 1988.

Garland, G. D., *Introduction to Geophysics* (*Mantle, Core and Crust*), 494 pp., W. B. Saunders, Philadelphia, Pa., 1979.

Gauthier, J. H., Unified structure in Quaternary climate, *Geophys. Res. Lett.*, *26*, 763–766, 1999.

Glatzmaier, G. A., and G. Schubert, Three-dimensional spherical models of layered and whole mantle convection, *J. Geophys. Res.*, *98*, 21,969–21,976, 1993.

Grossman, E. E., and C. H. Fletcher III, Sea level higher than present 3500 years ago on the northern main Hawaiian Islands, *Geology*, *26*, 363–366, 1998.

Gurnis, M., Large-scale mantle convection and the aggregation and dispersal of supercontinents, *Nature*, *332*, 695–699, 1988.

Gurnis, M., Phanerozoic marine inundation of continents driven by dynamic topography above subducting slabs, *Nature*, *364*, 589–593, 1993.

Gurnis, M., Sculpting the earth from inside out, *Scientific American*, *284*(March), 40–47, 2001.

Hager, B. H., R. W. Clayton, M. A. Richards, R. P. Comer, and A. M. Dziewonski, Lower mantle heterogeneity, dynamic topography and the geoid, *Nature*, *313*, 541–545, 1985.

Haq, B. U., J. Hardenbol, and P. R. Vail, Chronology of fluctuating sea levels since the Triassic, *Science*, *235*, 1156–1187, 1987.

Haq, B. U., J. Hardenbol, and P. R. Vail, Mesozoic and Cenozoic chronostratigraphy and cycles of sea level change, in *Sea Level Changes: An Integrated Approach*, edited by C. K. Wilgus et al., *Spec Publ. Soc. Econ. Paleontol. Mineral.*, *42*, 71–108, 1988.

Harrison, C. G. A., Modelling fluctuations in water depth during the Cretaceous, in *Fine-Grained Deposits and Biofacies of the Cretaceous Western Interior Seaway: Evidence of Cyclic Sedimentary Processes*, edited by L. M. Pratt, E. G. Kauffman, and F. B. Zelt, *SEPM Field Trip Guidebook*, *4*, 11–16, 1985.

Harrison, C. G. A., Eustasy and epeirogeny of continents on time scales between about 1 and 100 M. Y., *Paleoceanography*, *3*, 671–684, 1988.

Harrison, C. G. A., Constraints on ocean volume change since the Archean, *Geophys. Res. Lett.*, *26*, 1913–1916, 1999.

Harrison, C. G. A., G. W. Brass, E. Saltzman, J. Sloan II, J. Southam, and J. Whitman, Sea level variations, global sedimentation rates and the hypsographic curve, *Earth Planet. Sci. Lett.*, *54*, 1–16, 1981.

Hernandez-Molina, F. J., L. Somoza, J. Rey, and L. Pomar, Late Pleistocene-Holocene sediments on the Spanish continental shelves: model for very high resolution sequence stratigraphy, *Mar. Geol.*, *120*, 129–174, 1994.

Hsui, A. T., K. A. Rust, and G. D. Klein, A fractal analysis of Quaternary, Cenozoic-Mesozoic, and Late Pennsylvanian sea level changes, *J. Geophys. Res.*, *98*, 21,963–21,967, 1993.

Imbrie, J., J. D. Hays, D. G. Martinson, A. McIntyre, A. C. Mix, J. J. Morley, N. G. Pisias, W. L. Prell, and N. J. Shackleton, The orbital theory of Pleistocene climate: support from a revised chronology of the marine ^{18}O record, in *Milankovitch and Climate, Part I*, edited by A. L. Berger et al., D. Reidel, Norwell, Mass., 1984.

Kauffman, E. G., Cretaceous marine cycles of the western interior, *Mt. Geol.*, *4*, 227–245, 1969.

Lithgow-Bertelloni, C., and M. Gurnis, Cenozoic subsidence and uplift of continents from time-varying dynamic topography, *Geology*, *25*, 735–738, 1997.

Mao, A., C. G. A. Harrison, and T. H. Dixon, Noise in GPS coordinate time series, *J. Geophys. Res.*, *104*, 2797–2816, 1999.

Muller, R. A., and G. J. MacDonald, Glacial cycles and astronomical forcing, *Science*, *277*, 215–217, 1997.

Press, W. H., B. P. Flannery, S. A. Teukolsky, and W. T. Vetterling, *Numerical Recipes The Art of Scientific Computing*, 818 pp., Cambridge Univ. Press, New York, 1986.

Radlinski, A. P., E. Z. Radlinska, M. Agamalian, G. D. Wignall, P. Lindler, and O. G. Randl, Fractal geometry of rocks, *Phys. Rev. Lett.*, *82*, 3078–3081, 1999.

Sloss, L. L., The tectonic factor in sea level change: A countervailing view, *J. Geophys. Res.*, *96*, 6609–6617, 1991.

Swart, P., M. Moore, C. Charles, and F. Böhm, Sclerosponges may hold new keys to marine paleoclimate, *Eos*, *79*, 633, 1998.

Swart, P. K., S. Thorrold, J. Rubinstone, B. Rosenheim, C. G. A. Harrison, M. Grammer, and C. Latkoczy, Intra-annual variation in the stable oxygen and carbon and trace element composition of sclerosponges, *Paleoceanography*, in press, 2002.

Turcotte, D. L., *Fractals and Chaos in Geology and Geophysics*, 2nd ed., 397 pp., Cambridge Univ. Press, New York, 1997.

Wunsch, C., Bermuda sea level in relation to tides, weather, and baroclinic fluctuations, *Rev. Geophys.*, *10*, 1–49, 1972.

Wunsch, C., Decade-to-century changes in the ocean circulation, *Oceanography*, *5*, 99–106, 1992.